
Performance of air cooled hydrogen storage device with external fins

G. Mohan, M. Prakash Maiya, and S. Srinivasa Murthy (corresponding author)
*Refrigeration and Air Conditioning Laboratory, Department of Mechanical Engineering,
Indian Institute of Technology Madras, Chennai-600 036, India.*
E-mail: ssmurthy@iitm.ac.in

Abstract Minimization of total weight is the major criterion in the design of a solid state hydrogen storage device for mobile or portable applications. The design should also address the requirements such as storage capacity, charge/discharge rates, space constraints, coolant temperature and hydrogen supply pressure. To achieve this, one should be able to reliably predict the dynamic performance of the storage device. In this paper, a parametric study of hydrogen sorption in an air-cooled annular cylindrical hydrogen storage device with external fins is reported. LaNi_5 , which has excellent hydrogen storage properties is used as the hydriding material. The influence of different geometric parameters such as hydride bed thickness and fin height, and operational parameters such as hydrogen supply pressure and cooling air temperature are studied.

Keywords LaNi_5 ; metal hydride; heat and mass transfer; simulation; hydrogen storage

Nomenclature

b	bed thickness [m]
C_p	specific heat [$\text{J kg}^{-1} \text{K}^{-1}$]
D	diffusivity [$\text{m}^2 \text{s}^{-1}$]
d	diameter [m]
E_a	activation energy [J mol^{-1}]
k	thermal conductivity [$\text{W m}^{-1} \text{K}^{-1}$]
k_B	Boltzmann constant [eV/K]
\dot{m}	hydrogen mass absorbed [$\text{kg m}^{-3} \text{s}^{-1}$]
p	pressure [Pa]
r	radial coordinate [m]
R	universal gas constant [$\text{J mol}^{-1} \text{K}^{-1}$]
s	pitch distance [m]
τ	time [s]
T	temperature [K]
u	velocity [m s^{-1}]

Greek Letters

ΔH^0	heat of formation [J kg^{-1}]
ε	porosity
μ	dynamic viscosity, $\text{kg m}^{-1} \text{s}^{-1}$
θ	polar coordinate, radian
ρ	density, kg m^{-3}

Subscripts

<i>b</i>	base
<i>c</i>	coolant
<i>e</i>	effective
<i>eq</i>	equilibrium
<i>f</i>	fin
<i>g</i>	gas
<i>i</i>	inside
<i>in</i>	inlet
<i>s</i>	solid
<i>sat</i>	saturated
<i>w</i>	wall
0	initial

1. Introduction

Metal hydride hydrogen storage devices possess several functional benefits which include high volumetric storage capacity, fast reaction kinetics, a large number of charge-discharge cycles and safety. Metal hydrides are formed on exposure of certain metals or alloys to hydrogen at ordinary temperatures and pressures. One of the major drawbacks inherent to metal hydride is the poor heat and mass transfer characteristics, which invite special attention to the design of the storage device. Solid state hydrogen storage devices contain a bed or matrix of storage material into which hydrogen is absorbed during the charging process. This exothermic process demands effective cooling of the adsorbent in order to achieve the desired storage capacity and charging rate. Depending on the application, the heat transfer medium can be either a liquid or a gas.

A large number of simulation studies reported in literature consider liquid cooled/heated hydrogen storage devices while those dealing with air-cooled/heated systems are scarce. Hajji and Khalloufi [1] reported that the metallic fins with lower contact resistance at the hydride-tube interface can significantly improve the sorption kinetics. MacDonald and Rowe [2, 3] studied the effects of external convection on the thermodynamic behaviour in a metal hydride tank. Their preliminary resistive analysis suggested that the addition of external fins on the tank could have a significant impact on the overall heat transfer. This was verified by a numerical model, which revealed that when hydrogen is discharged by a pulsed mass flow rate demand, a finned tank is able to maintain a higher supply pressure. Another interesting observation made in this study was that the hydride in the centre region contributes little to fuel delivery, and removing it would reduce the weight and cost of the system. The paper presented here takes this observation into account by the introduction of a filter in the center of the tube. A parametric study of an air-cooled annular cylindrical hydrogen storage device with external fins, highlighting the influence of different geometric and operational parameters is reported here.

2. Physical Model

The annular cylindrical storage device shown in Fig. 1 consists of a porous sintered filter element (in practice 1–2 micron pore size) located at the centre for uniform distribution of hydrogen. The stainless steel container tube has external aluminum fins which transfer the exothermic heat generated to the surrounding air stream. Hydrogen gas introduced into the device through the filter gets absorbed in the alloy releasing heat. The absorption process will be faster close to the periphery of tubes and those regions will be saturated earlier than the rest. One can visualize a smooth interface, known as a reaction front which demarcates the fully hydrided portion from the rest of the unsaturated regions. As time proceeds, the reaction front moves inward from the periphery of the tubular device to the unsaturated areas of the alloy near the filter.

The exact mathematical formulation of heat and mass transfer mechanism within the metal hydride bed is difficult due to the unpredictable nature of alloy material. Various assumptions made for the simplified treatment of the problem are listed below.

- i. Hydrogen is treated as an ideal gas as the pressure within the bed is moderate.
- ii. Plateau slope and hysteresis factors for LaNi_5 are too small to have a significant effect on absorption [4]. Therefore, the effect of hysteresis and plateau slope for LaNi_5 is not accounted in simulation.

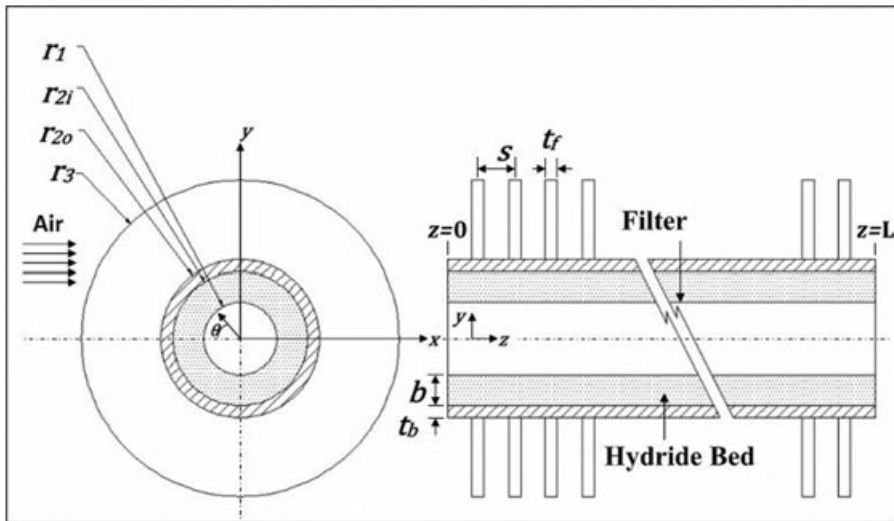


Figure 1. Schematic diagram of tubular metal hydride storage device with external fins.

- iii. Pressure variation and associated gas movement inside the metal hydride bed is not very significant and the effect of convection inside the bed is negligibly small. LaNi₅ is a low temperature hydriding alloy. So, radiation heat transfer inside the bed is not significant [5]. So, conduction is the prominent mode of heat transfer within the bed.
- iv. The hydride bed is assumed to have uniform porosity. Brittle metal hydride materials upon cyclic hydrogenation asymptotically reach a minimum particle size [6]. Therefore, the effect of powdering and variation in porosity is more pronounced in the early stages of absorption. After a certain number of charge-discharge cycles, the variation in porosity with time is insignificantly small.
- v. The hydride bed is assumed to be a homogeneous and isotropic porous media where permeability, effective thermal conductivity and mass diffusivity of the bed are independent of position and direction.
- vi. Local thermal equilibrium is assumed between the gas and solid within the bed. Non-local thermal equilibrium effects are confined to the reactor wall and hydrogen filters. However its overall effect on the performance of the device is minimal [7]. In most bulk portions of the bed, local thermal equilibrium is still valid. So it may be justified in simulation.
- vii. Thermo-physical properties such as thermal conductivity, dynamic viscosity and permeability of the bed are considered independent of bed temperature, pressure and concentration.

3. Problem Formulation

3.1 Mass balance of metal

Hydrogen entering the alloy bed through filters is absorbed forming the metal hydride. Transient changes in hydride density are attributed to both absorption reaction and diffusive transport due to spatial variation in concentration. As listed under assumptions, a constant value of porosity is taken. Conservation of mass for the solid phase of the reactor in cylindrical coordinates is expressed in the following form:

$$(1-\varepsilon)\frac{\partial \rho_s}{\partial \tau} = \dot{m} + (1-\varepsilon)D\frac{1}{r}\frac{\partial}{\partial r}\left(r\frac{\partial \rho_s}{\partial r}\right) + (1-\varepsilon)D\frac{1}{r^2}\frac{\partial}{\partial \theta}\left(\frac{\partial \rho_s}{\partial \theta}\right) + (1-\varepsilon)D\frac{\partial}{\partial z}\left(\frac{\partial \rho_s}{\partial z}\right) \quad (1)$$

Diffusivity D may be represented by the Arrhenius expression [8].

$$D = D_0 \exp\left(\frac{-H_a}{k_B T}\right) \quad (2)$$

Where H_a represent activation enthalpy and k_B is the Boltzmann constant.

Transient variation in density on the left hand side is expressed as the sum of four terms on the right hand side. The first term represents the mass of hydrogen absorbed due to reaction. The remaining terms of the equation signify the effect of diffusive transport due to the concentration gradients existing within the bed. Convection term is neglected in eqn. (1).

3.2 Absorption kinetics

The amount of hydrogen absorbed is directly related with the reaction rate, and could be given as below:

$$\dot{m} = -C_a \exp\left(-\frac{E_a}{RT}\right) \ln\left(\frac{P}{P_{eq}}\right) (\rho_{sat} - \rho_s) \quad (3)$$

where C_a is a material dependent constant, E_a is the activation energy of the material, ρ_{sat} is the density of hydride at saturation. The change in volume if any, due to hydrogen absorption, is not considered in the computation of the density of the bed. The equilibrium pressure is determined by the van't Hoff relationship as given below:

$$\ln P_{eq} = A - \frac{B}{T} \quad (4)$$

where A and B are van't Hoff constants.

3.3 Energy balance

Heat generated due to exothermic reaction causes associated spatial temperature imbalances within the bed. The energy conservation equation of the bed could be expressed as below:

$$(\rho C_p)_e \frac{\partial T}{\partial \tau} = k_e \frac{1}{r} \frac{\partial}{\partial r} \left(r \frac{\partial T}{\partial r} \right) + k_e \frac{1}{r^2} \frac{\partial}{\partial \theta} \left(\frac{\partial T}{\partial \theta} \right) + k_e \frac{\partial}{\partial z} \left(\frac{\partial T}{\partial z} \right) - \dot{m} \Delta H^0 \quad (5)$$

Equation (5) assumes the existence of local thermal equilibrium between the solid and gas within the bed. Hence the heat transfer between the two phases is omitted. Radiation heat transfer to the ambient is also neglected. Heat of formation of hydride represents the source term in the above equation.

Effective volumetric heat capacity is represented by the following expression:

$$(\rho C_p)_e = (\epsilon \rho_g C_{pg} + (1 - \epsilon) \rho_s C_{ps}) \quad (6)$$

Effective thermal conductivity is expressed as given below:

$$k_e = \epsilon k_g + (1 - \epsilon) k_s \quad (7)$$

3.4 Initial and boundary conditions

Initially the pressure and temperature of the reactor bed are assumed to be uniform. Therefore,

$$p = p_0; \quad T = T_0; \quad \rho = \rho_0 \quad \text{at} \quad \tau = 0 \quad (8)$$

The boundary walls of the reactor are assumed to be impermeable and adiabatic. The reaction heat is removed from the porous bed by passing the air stream over the tubular device. 'No slip condition' is valid at the reactor wall and fins. Hydrogen is supplied through the porous filter tubes. Convective flux conditions prevail at the filter walls which are assumed to be adiabatic. Based on the above assumptions, the following boundary conditions may be applied to the metal hydride bed bounded with reactor and filter walls:

Reactor wall at $r = r_{2i}$; $0 \leq z \leq L$:

$$\frac{\partial p}{\partial r} = 0; \quad -k_e \frac{\partial T}{\partial r} = -k_w \frac{\partial T_w}{\partial r} \quad \text{at} \quad \tau > 0 \quad (9)$$

Since the subdomains, base tube-fluid and fin-fluid are coupled, continuity of heat flux condition is assumed at the interface boundaries. Further, no slip conditions hold good at all solid-fluid interfaces for fluid flow.

4. Simulation Methodology

The simulation of the metal hydride bed employing the above mentioned partial differential equations were carried out using the commercial code COMSOL MULTIPHYSICS [9]. An unstructured mesh of suitable element size is generated by defining appropriate mesh parameters. Four different sub-domains which include the metal hydride bed, base tube, fin and fluid stream were modeled using the geometry modeling features of the software. Subsequently, relevant physics and material properties were applied to each domain. The equations across different sub-domains are appropriately coupled using the inbuilt features of the software. Different governing equations used for the present simulation include the convection-diffusion, non-isothermal flow and general heat transfer, applicable to different subdomains based on the degree of relevance. Application of convection-diffusion equation is limited to metal hydride subdomain where as non-isothermal flow holds good for the fluid stream. General heat transfer equation is applicable to all sub-domains.

5. Results and discussion

Results are computed for LaNi_5 as the hydriding material. The reaction rate for LaNi_5 is extremely fast and the alloy performance is limited by heat transfer in most applications. Role of intrinsic chemical kinetics is limited. Moreover it is well characterized. So the choice of LaNi_5 as the hydriding alloy in the present simulation

Table 1. *Thermo-physical properties of LaNi₅ and hydrogen [8, 10]*

Parameter	LaNi ₅	Hydrogen
Density, kg m ⁻³	8,200	0.0838 at NTP
Specific heat, J kg ⁻¹ K ⁻¹	419	14.890
Effective thermal conductivity, W m ⁻¹ K ⁻¹	1.2	0.12
Activation energy, J mol ⁻¹	21,179.6	–
Constants in eqns. (2), (3), (4): D ₀ (m ² /s)	3.4 × 10 ⁻⁷	–
H _a (eV)	0.29	–
C _a	59.187	–
A	12.99	–
B	3,704.59	–

Table 2. *Parameter values used in the present simulation study*

Parameter	Range of values
Initial temperature of hydride bed, T ₀ (K)	293 (Constant)
Supply pressure of hydrogen, p (bar)	7.0–15.0
Coolant (air) temperature, T _c (K)	290–320
Velocity of air stream, u (m/s)	3.5
Porosity, ε	0.5 (Constant)
Bed thickness, b (mm)	2–6
Thickness of the base tube, t _b (mm)	2
Thickness of fin, t _f (mm)	2
Pitch distance, s (mm)	6
Fin height, L (mm)	3 (low-fin), 13(high-fin)

may be more apt in comparison with other alloys. Reaction kinetics and thermo-physical property data for LaNi₅ are readily available in literature and given in Table 1. The simulation is carried out for different operating parameters, the ranges of which are given in Table 2.

The main parameters which influence the mass transfer process in the hydride bed include the hydrogen gas pressure, hydride bed temperature and the hydrogen concentration. Metal hydrides generate a large amount of heat due to the exothermic hydride forming reaction. The reaction within the bed is proportional to the differential between the gas supply pressure and equilibrium pressure corresponding to the bed temperature. While the supply pressure remains constant, the reactions become more vigorous when the bed temperature and the corresponding equilibrium pressure are lower. The bed temperature increases rapidly during the initial phase of the reaction. Heat transfer from the bed to the cooling media dissipates the heat generated in the process. Since the thermal diffusion process is comparatively slower than the chemical reaction, the hydriding rate drops as time progresses.

Exothermic heat generated within the bed during absorption is being carried away by the air stream flowing over the tubular device. Heat transfer to the surrounding

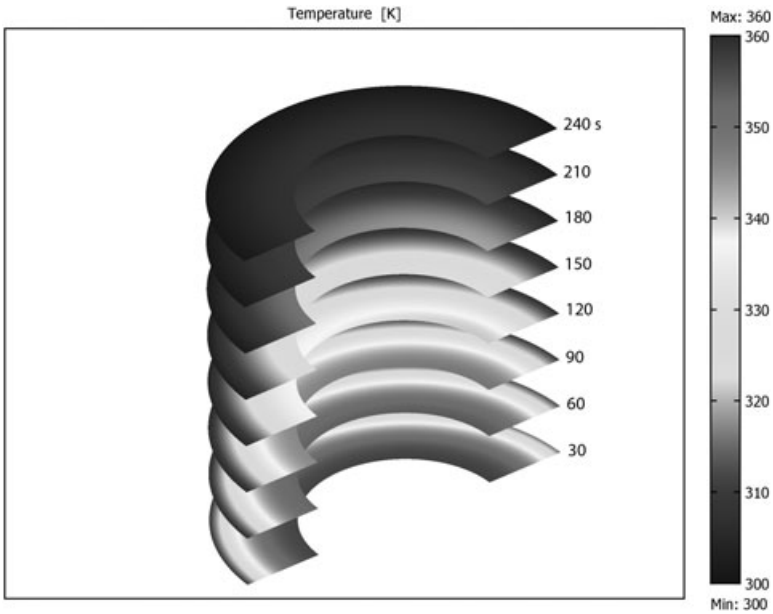


Figure 2. *Temperature profiles of metal hydride bed at selected time intervals.*

air stream is enhanced by means of fins. Convective heat transport by means of air at different spatial locations is attributed to the nature of the flow field. Figure 2 shows the slice plots of temperature profile of the metal hydride bed at different time intervals. At the initial phase of reaction the exothermic heat generation will be excessive which causes a rapid rise in temperature within the bed. Later, the rate of reaction is controlled by the heat transfer to the surrounding media, which causes a gradually decreasing temperature within the bed.

Figure 3 depicts the concentration profiles within the hydride bed. The reaction front progresses relatively faster during the early stages of absorption and becomes more and more sluggish with elapsed time, mainly attributed to the increasing conduction path length and poor heat transfer. It also shows the temperature profile of the surrounding flow field. The rate of removal of heat is more during the early stages as depicted in figure, further indicative of the higher rate of reaction.

Heat transfer from the device shows some disparity between the leading and trailing regions, owing to the heat pickup of the air stream as it flows along. Therefore development of reaction fronts shows a non uniform distribution i.e., higher rate of absorption in the leading half compared to the trailing half of the bed. Figure 4 shows the temperature variation across two different cross sections at angles 0 and 180 degrees during different time intervals. Even though the two plots exhibit similar

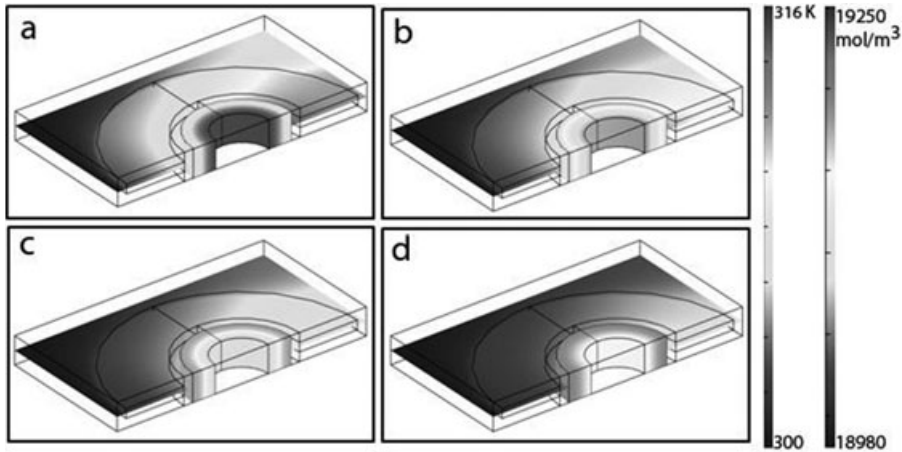


Figure 3. Formation of hydride inside tubular storage device with fins kept within the air stream during absorption at different time intervals a) 30 s b) 60 s c) 90s d) 120s ($b = 5 \text{ mm}$, $p = 15 \text{ bar}$, $T_c = 300 \text{ K}$).

trends, the temperature profile at $\theta = 0$ show lower bed temperature compared to $\theta = 180^\circ$. The differences are more evident during the initial phase of reaction and near the finned wall where the reaction rates are more predominant.

A lower bed temperature essentially lowers the corresponding equilibrium pressure within the device, which enhances the rate of hydrogen sorption within the bed. Figure 5 shows the rate of hydrogen sorption at two different cross sections at angles 0 and 180 respectively. At the initial stages of reaction there exists a disparity in absorption between the finned wall and filter wall which is clearly evident from the above figure. At the later stages the above disparity fades out, which may be an indication that the reaction becomes more heat transfer controlling. Still the disparity between the leading and trailing halves may be observed at locations where the reaction is more vigorous. The plots depicts a progressive wave front behaviour from tube wall to the filter wall indicative of the progressing reaction front moving across the cross section.

Figure 6 depicts time varying profiles of hydride density across the bed at two different cross sections at angles 0 and 180 degrees respectively. Hydride density at the finned wall is obviously high at all different cases. The rate of increase in density is higher at the initial stages of reaction and becomes more and more sluggish at the ending stage. Both plots exhibit similar behavior barring the usual disparity between the leading and trailing halves.

Bed thickness has been recognized as an important geometric parameter that influences the performance of any hydrogen storage device. For thinner beds, the conduction path is relatively short. If thickness exceeds an optimum value, the gain

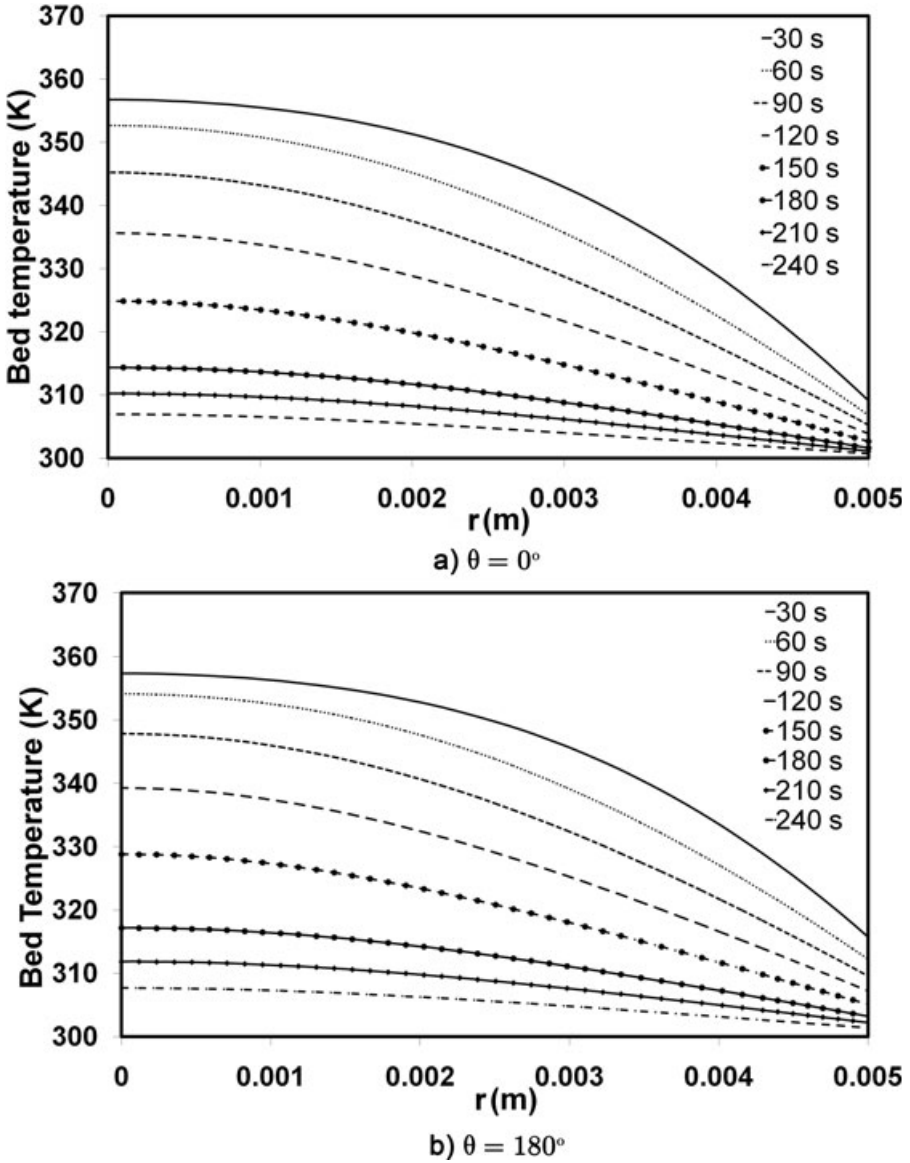


Figure 4. Profiles of temperature variation across the bed at different radial distances from filter and two different angles a) $\theta = 0^\circ$ b) $\theta = 180^\circ$ ($b = 5$ mm, $p = 15$ bar, $T_c = 300$ K).

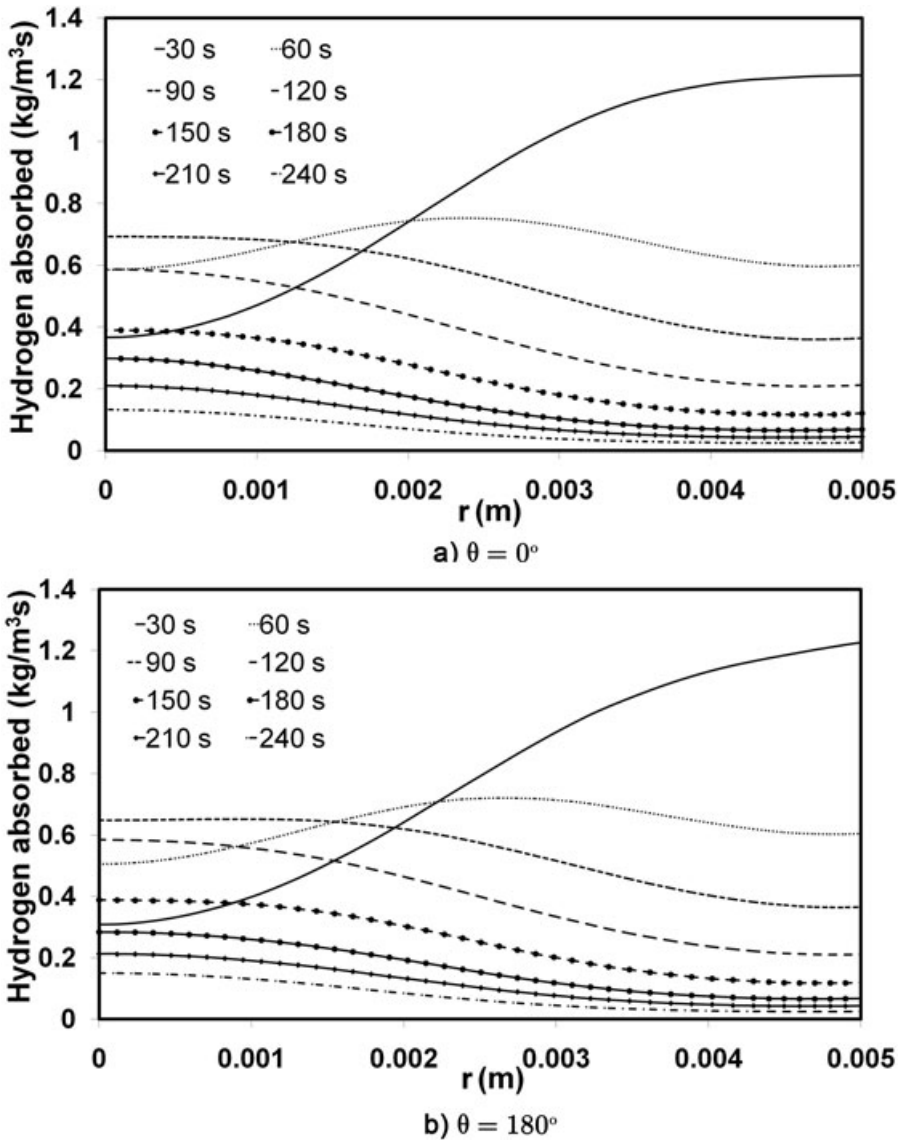


Figure 5. Profiles of hydrogen absorption across the bed at different radial distances from filter and two different angles a) $\theta = 0^\circ$ b) $\theta = 180^\circ$ ($b = 5 \text{ mm}$, $p = 15 \text{ bar}$, $T_c = 300 \text{ K}$).

Downloaded from https://academic.oup.com/ijlct/article-abstract/3/4/265/7638993 by guest on 10 June 2020

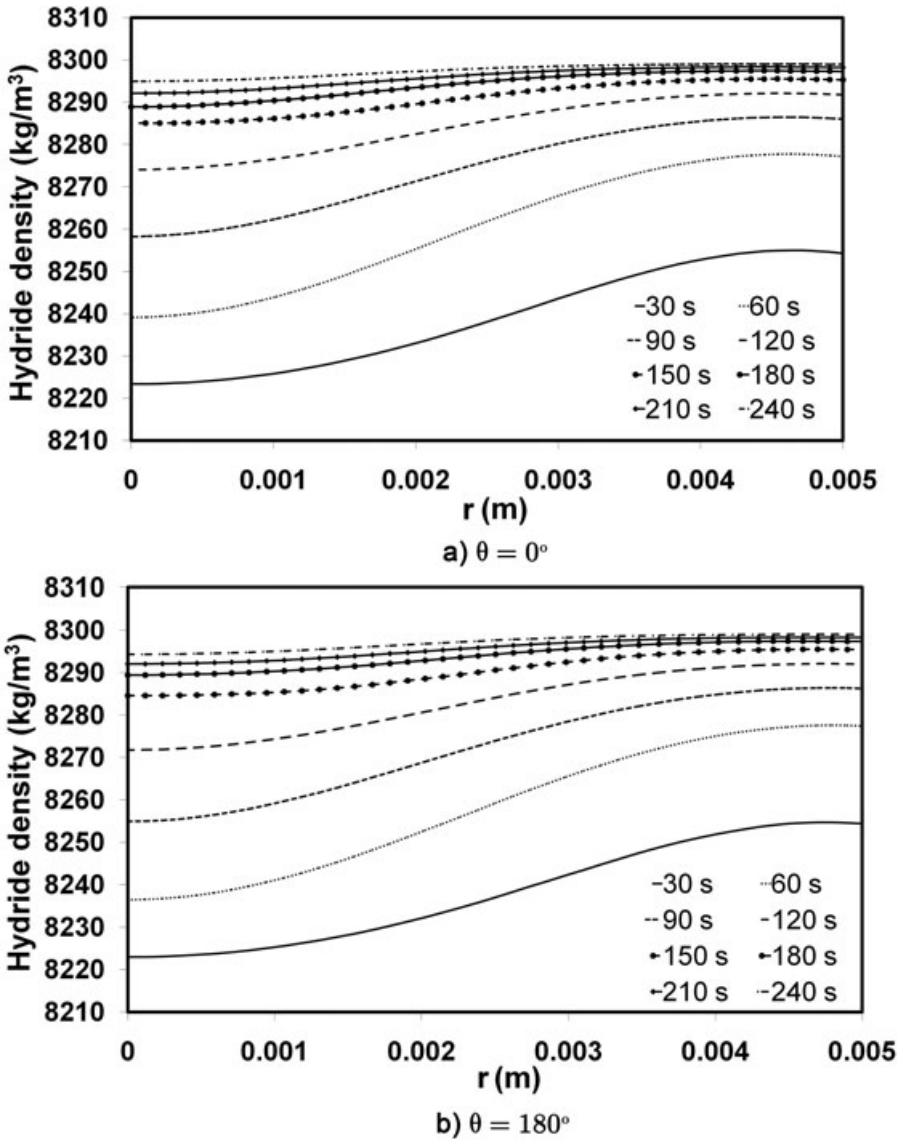


Figure 6. Profiles of hydride density across the bed from filter at different radial distances and two different angles a) $\theta = 0^\circ$ b) $\theta = 180^\circ$ ($b = 5 \text{ mm}$, $p = 15 \text{ bar}$, $T_c = 300 \text{ K}$).

Downloaded from https://academic.oup.com/ijlct/article-abstract/3/4/265/7638993 by guest on 10 June 2020

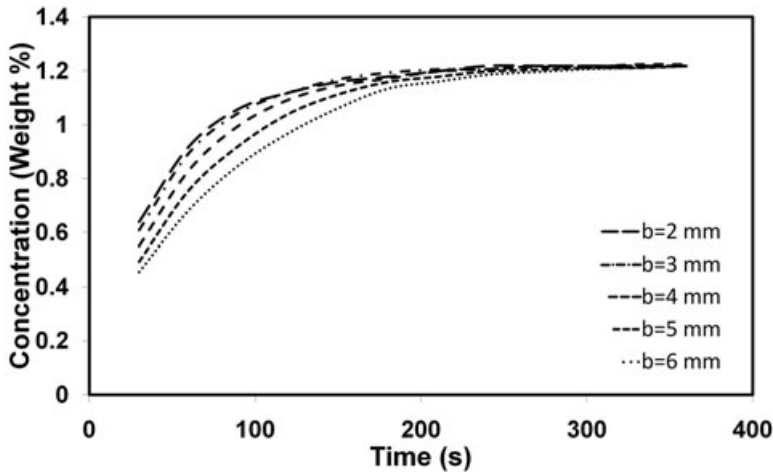


Figure 7. Effect of bed thickness on hydride formation ($p = 15$ bar, $T_c = 300$ K).

due to a higher quantity of hydride is negated by the increased conduction resistance to heat transfer. At specified conditions of cooling media temperature and pressure, the rate of absorption depends on bed thickness. Figure 7 shows the influence of bed thickness on absorption of hydrogen.

In all cases, the same saturated state of approx. 1.2 weight % H_2 is achieved after different time intervals. At a lower bed thickness of $b = 2$ mm, the hydride bed reaches saturation earlier than others leading to lower cycle time. Higher bed thicknesses result in flatter profiles and take a longer time to reach the saturation state. Higher bed temperature, lower reaction rate, larger conduction path length and low thermal conductivity material are collectively important for the above described phenomena. For a given bed thickness, heat transfer as well as reaction kinetics are jointly important in determining the absorption time. As reaction kinetics is more material dependent, for a specified effective thermal conductivity value, there exists an optimum bed thickness satisfying the prescribed performance and system weight.

Heat transfer augmentation is always important in the design of metal hydride devices. Figure 8 shows the absorption rates with and without fins. The device with fins shows a visible improvement in heat transfer over the one with no fin, leading to higher rates of absorption. High finned tubes leads to lower equilibrium pressures within the bed, which causes higher pressure differential and sorption rates. It may be noted further that the performance improvement of the high-fin (13 mm) tube over the low-fin (3 mm) tube is small. Moreover maintenance of low finned tubes is easier in applications where soot deposition is problematic. So low fin tubes may be preferred for applications where reduction in system weight is important and flue gases are used as the heat transfer media.

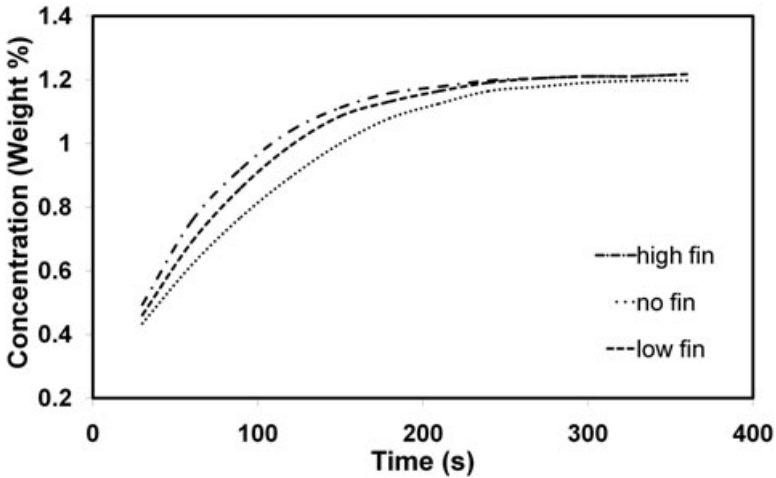


Figure 8. Effect of external fins on rate of hydriding ($b = 5$ mm, $p = 15$ bar, $T_c = 300$ K).

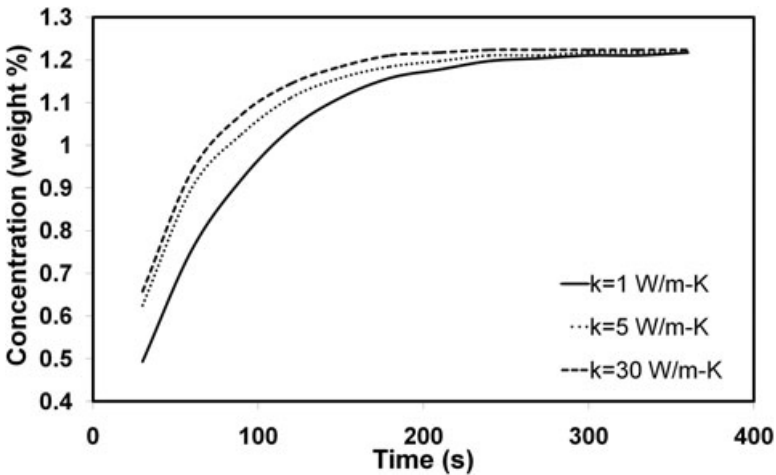


Figure 9. Effect of thermal conductivity of hydride bed on rate of hydriding ($b = 5$ mm, $p = 15$ bar, $T_c = 300$ K).

Figure 9 shows the effect of the thermal conductivity of the bed on the rate of hydriding. Increasing the thermal conductivity of the hydride bed improves the rate of the hydriding process. However, marginal improvement is observed for thermal conductivity beyond 5 W/m-K. The above characteristic is indicative of the mutual correlation between reaction kinetics, internal and external resistance to heat transfer in controlling the rate of hydrogen sorption. Fast reaction kinetics should be

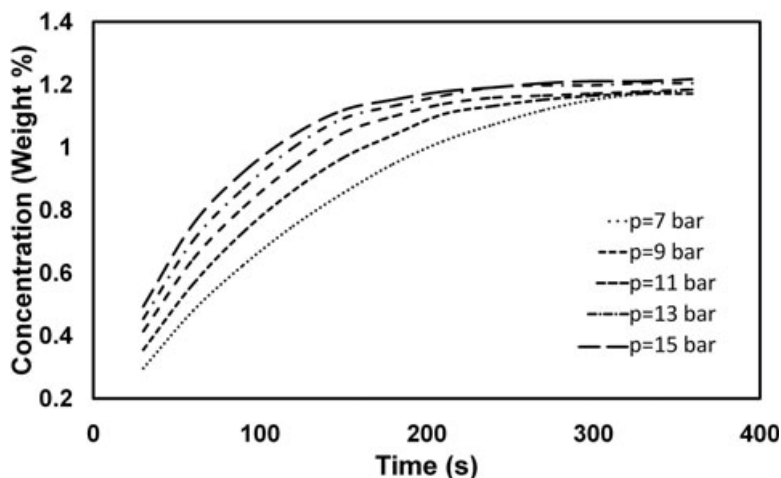


Figure 10. Effect of supply pressure on hydrogen sorption ($b = 5$ mm, $T_c = 300$ K).

accompanied with suitably lower heat transfer resistances both within and external to the bed.

There are two major operational parameters which control the overall performance of the device, namely, system supply pressure and surrounding coolant media (air) temperature. Supply pressure is an extremely important operating parameter controlling the hydriding rates. The pressure differential between equilibrium pressure and imposed pressure within the reactor controls the rate of absorption process. A higher pressure differential reduces the cycle time as illustrated in Fig. 10. Cooling media temperature is a major parameter in controlling the temperature of the bed. The effect of cooling media temperature on hydriding is shown in Fig. 11. At any given supply pressure, lower coolant temperature causes a lower bed temperature and thereby lower equilibrium pressure. It consequently increases the driving potential for mass transfer, resulting in a higher rate of reaction.

6. Conclusions

Heat and mass transfer simulation of an air cooled hydrogen storage device with external fins is carried out with LaNi_5 as the alloy material for different geometric parametric ranges and operational conditions. Results of the simulation show the existence of disparity in hydriding rates between the leading and trailing halves of the device. The above disparity is more pronounced during the early stages of reaction when the reaction rate is high. The results confirm the importance of bed thickness as the major geometric parameter controlling the rate of hydrogen absorption within the bed. External fins and thermal conductivity enhancement of the metal hydride bed improves the rate of hydrogen sorption. However, the effect of fin height

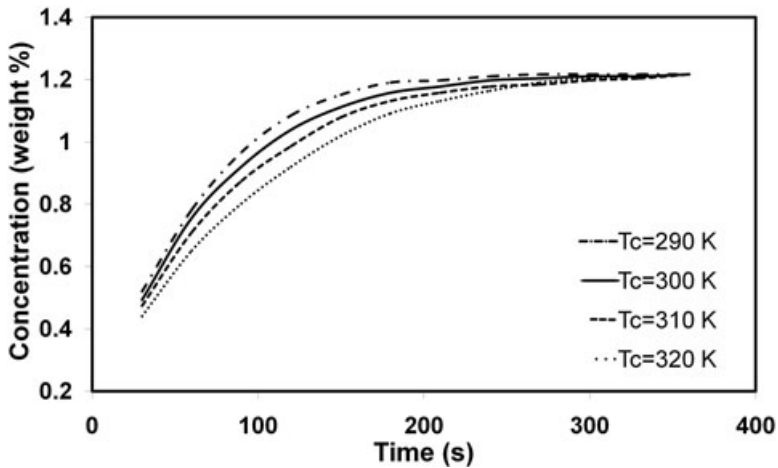


Figure 11. Effect of coolant (air) temperature on hydride formation ($b = 5$ mm, $p = 15$ bar).

on the overall performance is minimal. Hydrogen pressure within the bed is an important operational parameter influencing the rate of hydriding within the bed. Temperature of air stream passing over the tubular device influences the overall hydriding performance of the device to a reasonable extent.

Acknowledgements

The financial support from U.S. Army Communications – Electronics Research, Development and Engineering Center, and International Technology Center – Pacific are gratefully acknowledged.

References

- [1] A. Hajji and S. Khalloufi, 'Improving the performance of adsorption heat exchangers using finned structure', 39(8) (1996), 1677–1686.
- [2] B. D. MacDonald and A. M. Rowe, 'Impacts of External Heat Transfer Enhancements on Metal Hydride Storage Tanks', *International Journal of Hydrogen Energy*, 31(12) (2006), 1721–1731.
- [3] B. D. MacDonald and A. M. Rowe, 'A Thermally Coupled Metal Hydride Hydrogen Storage and Fuel Cell System', *Journal of Power Sources*, 161(1) (2006), 346–355.
- [4] (<http://www.hydpark.ca.sandia.gov>) Hydride Information Centre, Sandia National Laboratories, USA.
- [5] F. Askri, A. Jemni and S. B. Nasrallah, 'Study of Two Dimensional and Dynamic Heat and Mass Transfer in a Metal Hydride Bed', *International Journal of Hydrogen Energy*, 28 (2003), 537–557.

- [6] M. Ron, 'The Normalized Pressure Dependence Method for the Evaluation of Kinetic Rates of Metal Hydride Formation/Decomposition', *Journal of Alloys and Compounds*, 283 (1999), 178–191.
- [7] G. M. Lloyd, A. Razani and K. J. Kim, 'Formulation and Numerical Solution of Non-local Thermal Equilibrium Equations for Multiple Gas/Solid Porous Metal Hydride Reactors', *Transactions of the ASME-Journal of Heat Transfer*, 123 (2001), 520–526.
- [8] G. Majer, U. Kaess and R. C. Bowman Jr., 'Nuclear Magnetic Resonance Studies of Hydrogen Diffusion in $\text{LaNi}_{5.0}\text{H}_{6.0}$ and $\text{LaNi}_{4.8}\text{Sn}_{0.2}\text{H}_{5.8}$ ', *Physical Review B*, 57 (1998), 21, 599–603.
- [9] Comsol Multiphysics User's Guide. 2005. Comsol AB, Sweden.
- [10] A. Dogan, Y. Kaplan and T. N. Veziroglu, 'Numerical Investigation of Heat and Mass Transfer in a Metal Hydride Bed', *Applied Mathematics and Computation*, 150(1) (2004), 169–180.